

Localization of ferrocene in NaY zeolite by powder x-ray and neutron diffraction

E. Kemner,^{a)} A. R. Overweg, and L. van Eijck

Interfaculty Reactor Institute, Delft University of Technology, Mekelweg 15, 2629 JB Delft, The Netherlands

A. N. Fitch

European Synchrotron Radiation Facility, BP 220, F-38043 Grenoble Cedex 9, France

E. Suard

Institut Laue Langevin, BP 156, F-38042 Grenoble Cedex 9, France

I. M. de Schepper and G. J. Kearley

Interfaculty Reactor Institute, Delft University of Technology, Mekelweg 15, 2629 JB Delft, The Netherlands

(Received 3 January 2002; accepted 27 March 2002)

We study the inclusion of the metallocene ferrocene $\text{Fe}(\text{C}_5\text{H}_5)_2$ molecules in the supercages of NaY zeolite. To find the exact location of the ferrocene molecules within the supercages we perform neutron and powder x-ray diffraction on bare NaY zeolite, and on NaY zeolite loaded with one or two ferrocene molecules per supercage. Using the complementary properties of both techniques we show that the ferrocene molecules are located just above a line joining two neighboring sodium ions at the SII positions in the zeolite supercage. The C_5H_5 rings are oriented towards the sodium ions in an ordered manner. This structure is confirmed by quantum chemistry calculations. The geometry of the ferrocene molecules barely changes, indicating that the increased reactivity of ferrocene upon adsorption in a zeolite is thus a result of the position of the molecules. The main interactions responsible for this position are Coulombic attraction and hydrogen bonding. The inclusion of ferrocene in a Y-type zeolite provides a homogeneous distribution of iron throughout the zeolite at well-defined locations. © 2002 American Institute of Physics. [DOI: 10.1063/1.1479713]

I. INTRODUCTION

Zeolites are crystalline aluminosilicates with a three-dimensional open framework structure of channels and cavities of molecular dimensions. Zeolites can thus act as molecular sieves, making catalytic centers in the interior of the zeolite only accessible to molecules of the correct size. An extensively used type of zeolite is the faujasite or Y-type zeolite, which has especially large cavities, called supercages. These have a diameter of about 12 Å and are interconnected through windows with a diameter of 9 Å. The traditional way of introducing catalytic centers in such zeolites is ion exchange. The disadvantages of this method are undesired oxidation states of the ions and their unwanted final locations (i.e., not in the supercages) in the zeolite. An alternative to ion exchange is vapor phase insertion of volatile compounds, such as organometallics, that contain the catalytically active ions. Metal carbonyls are particularly favored because they contain metals in a zerovalent oxidation state and the carbonyl ligands can be removed under mild conditions after insertion of the compound in the zeolite. This makes the formation of neutral metal clusters possible. Moreover, the metal will also be deposited in the supercages only, where it is wanted to perform the desired catalytic activity. Because of these future prospects of applications in

heterogeneous catalysis confinement of organometallics in the voids of zeolite host frameworks has gained considerable attention over the last years.^{1–5}

For a fundamental understanding of these systems knowledge of the interaction between the organometallic guest molecules and the zeolite host framework is desired. We use the relatively simple organometallic ferrocene, $\text{Fe}(\text{C}_5\text{H}_5)_2$, adsorbed in the supercages of NaY zeolite, $\text{Na}_x(\text{AlO}_2)_x(\text{SiO}_2)_{192-x}$, as a model system. Ferrocene consists of an iron atom “sandwiched” by two identical parallel cyclopentadienyl C_5H_5 rings with a radius of 2.3 Å, separated by approximately 3.3 Å. The supercages of NaY zeolite contain four sodium ions on the surface of the framework, on the so-called SII positions (see Fig. 1). The inclusion of ferrocene in the voids of zeolites has been investigated before (see Ref. 4, and references therein). One remarkable effect found is that unlike pure ferrocene in the solid or gas-phase state, ferrocene in zeolite Y oxidizes quite easily.^{1,4}

To fully understand the interaction between the ferrocene molecules and the zeolite framework, knowledge of the location of ferrocene in the zeolite host is required. In the present study we determine the location of ferrocene in NaY zeolite by means of powder x-ray and neutron diffraction at a temperature $T=10$ K and $T=1.5$ K, respectively, for loadings of one and two ferrocene molecules per supercage. Using the complementary properties of both techniques we show that the ferrocene molecules are located just above a line joining two neighboring sodium ions at the SII positions in the zeolite supercage with the C_5H_5 rings oriented towards

^{a)} Author to whom correspondence should be addressed. Telephone: +31 152787109; fax: +31 152788303; electronic mail: kemner@iri.tudelft.nl

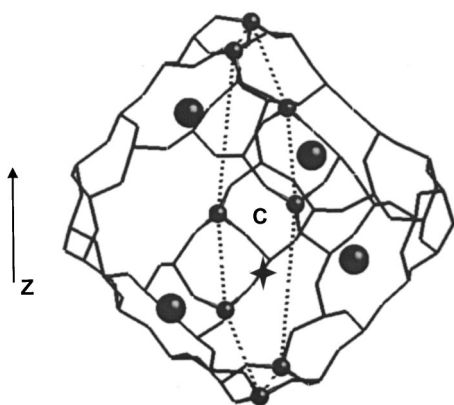


FIG. 1. The supercage of NaY zeolite. The framework (solid line) is formed from silicon, aluminum, and oxygen atoms. The cage contains four sodium ions (large dots) at the SII positions. The dashed line connecting 8 silicon/aluminum atoms (small dots) gives the plane for which we show a Fourier difference map in Fig. 3. The C represents the center of the supercage, the cross the position of an iron atom as determined from Fig. 3.

the sodium ions in an ordered manner for loadings with one and two ferrocene molecules per supercage. Ferrocene is thus homogeneously distributed throughout the zeolite at well-defined locations. The geometry of the ferrocene molecules themselves barely changes, indicating that the increased reactivity of ferrocene upon adsorption in a zeolite is thus a result of the position of the molecules. The main interactions responsible for this position and orientation are electrostatic attraction and hydrogen bonding.

II. EXPERIMENT

The unit cell composition of the NaY zeolite, when dehydrated, is $\text{Na}_{55}(\text{AlO}_2)_{55}(\text{SiO}_2)_{137}$. The zeolite was first dehydrated. For the x-ray diffraction experiments the bare zeolite was then loaded with ferrocene $\text{Fe}(\text{C}_5\text{H}_5)_2$, in a way similar as described by Overweg *et al.*,⁵ with an amount of ferrocene corresponding to one and two ferrocene molecules per supercage. After loading, the samples were transferred under nitrogen atmosphere in glass capillaries with a diameter of 1.0 mm, which were then sealed.

Because of the high incoherent scattering cross section of hydrogen we used deuterated ferrocene $\text{Fe}(\text{C}_5\text{D}_5)_2$ for the neutron diffraction experiments. The zeolite was loaded with deuterated ferrocene in the same way as described above, and the samples were transferred under nitrogen atmosphere into vanadium cylinders with a diameter of 7 mm which were sealed with indium.

Powder x-ray diffraction was performed at the BM16 diffractometer of the ESRF in Grenoble, France. We measured NaY zeolite loaded with one and two ferrocene molecule per supercage at a temperature $T=10$ K. Dehydrated bare NaY zeolite was also measured, at a temperature $T=300$ K. The wavelength of the synchrotron radiation was 0.803 157 Å. The x-ray diffraction patterns were collected for 2θ angles from 0° until 78° . Powder neutron diffraction was performed at the D2b diffractometer of the ILL in Grenoble, France. We measured NaY zeolite loaded with one and with two deuterated ferrocene molecules at a temperature $T=1.5$ K. Dehydrated bare NaY zeolite was measured at

room temperature. The wavelength of the neutrons was 2.398 Å. Neutron diffraction patterns were collected for 2θ angles from 0° until 158° .

The data were analyzed by the Rietveld method using the program WINMPROF.⁶ The unit-cell, zero-point, overall scale factor, peak-width, asymmetry and background parameters were refined simultaneously with the structural and thermal parameters. Isotropic thermal parameters were used for all atoms.

III. STRUCTURE DETERMINATION

The structure of the bare NaY zeolite that we determine from x-ray and neutron diffraction at room temperature is found to be consistent with that obtained from earlier x-ray and neutron diffraction studies.⁷ The spacegroup is Fd3m. The observed, calculated, and difference profiles for bare NaY zeolite are shown in Figs. 2(a) and 2(b) for the neutron and x-ray data, respectively. For clarity we show part of the diffraction patterns only. The final structural parameters to which the refinements converged are shown in Tables I(a) and I(b).

We observe no symmetry changes due to the insertion of ferrocene in the zeolite. An initial refinement on the x-ray diffraction pattern of one ferrocene molecule per zeolite supercage using only the atoms of the zeolite framework and the sodium ions gave an unsatisfactory fit. This means that the ferrocene molecules contribute significantly to the diffraction pattern. We calculated Fourier difference maps with the program GFOUR (Ref. 8) using the observed intensities of the peaks for the pattern on zeolite loaded with ferrocene and those calculated for bare zeolite by WINMPROF. These maps then give the missing scattering density (electron density in case of x-ray scattering) in the calculated fit projected on real space. The Fourier difference map on the plane perpendicular to the $[0,1,0]$ axis about the center of the supercage located at $(3/8, 3/8, 3/8)$ is shown in Fig. 3. This plane and the zeolite framework atoms that lie in it are also indicated in Fig. 1. There are four spots in this map around the center of the supercage with significant missing electron density, which we contribute to the presence of iron atoms. Note that although only one ferrocene molecule is present in the supercage, the Fourier map gives more positions because it gives all other positions, which are symmetrically the same. After insertion of iron on these positions in the refinement, the refinement improved, and the spots disappeared in subsequent Fourier difference maps, meaning that the missing electron density indeed corresponded to the presence of iron atoms. One of these iron atoms is depicted with a cross in Fig. 3, and this location is also given by the cross in Fig. 1.

Fourier difference maps calculated from a refinement on the neutron data on one ferrocene molecule per supercage at 1.5 K using the zeolite framework, the sodium ions and iron at the position as found above give the location of the cyclopentadienyl rings. In the final refinement the geometry of the ferrocene molecule was constrained according to the known geometry of a single (eclipsed) ferrocene molecule⁹ and only the z coordinate is refined. The final results of the refinements on one ferrocene molecule per supercage are shown in Figs. 4(a) and 4(b) and Tables II(a) and II(b) for the neutron

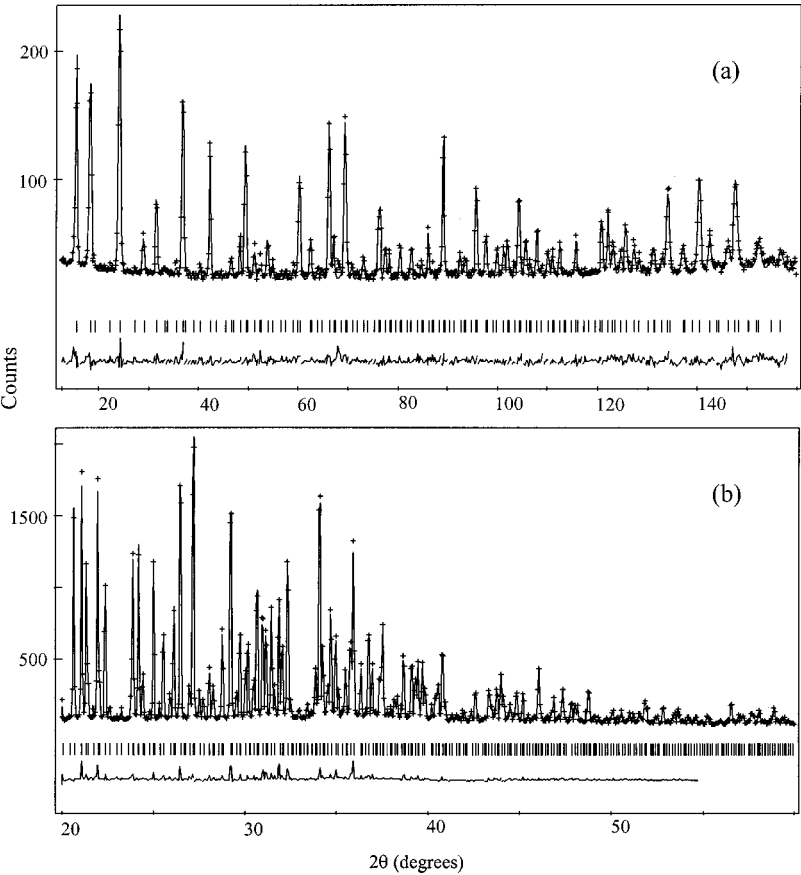


FIG. 2. Observed, calculated, and difference profiles for neutron powder diffraction (a) and x-ray powder diffraction (b) on bare dehydrated NaY zeolite.

and x-ray data, respectively. We do not include the hydrogen atoms of the cyclopentadienyl rings in the refinement on the x-ray pattern due to their very low scattering factor. Again we show only part of the patterns.

We observe no change in the positions of the ferrocene molecules for the case of two ferrocene molecules per zeolite supercage. The final structural parameters are given in Tables

III(a) and III(b), and the results of the refinements on the collected patterns are shown in Figs. 5(a) and 5(b). We had to exclude the region up to 20° containing three peaks in the refinement on the neutron data due to the presence of diffuse scattering. We find that the number of ferrocene molecules as found from the neutron pattern is less than the number of ferrocene molecules as determined from the preparation.

TABLE I. Final parameters and *R* factors obtained from a Rietveld refinement on neutron (a) and x-ray (b) powder diffraction on bare NaY zeolite.

	Atom	Position	<i>x/a</i>	<i>y/a</i>	<i>z/a</i>	<i>B</i> (Å ²)	<i>N</i>
(a)							
	Si/Al	192 i	−0.0547(2)	0.0348(3)	0.1250(3)	0.71(8)	192
	O(1)	96 h	0	−0.1061(2)	0.1061(2)	1.3(2)	96
	O(2)	96 g	−0.0025(2)	−0.0025(2)	0.1423(3)	2.0(2)	96
	O(3)	96 g	0.1770(2)	0.1770(2)	−0.336(3)	3.0(2)	96
	O(4)	96 g	0.1780(2)	0.1780(2)	0.3171(3)	2.8(2)	96
	Na(1)	32 e	0.2325(4)	0.2325(4)	0.2325(4)	2.2(5)	32(1)
	Na(2)	32 e	0.0563(8)	0.0563(8)	0.0563(8)	2.2(5)	13(1)
	Na(3)	16 c	0	0	0	2.2(5)	6.4(6)
<i>a</i> = 24.8150(2) Å, <i>R</i> _I = 6.33%, <i>R</i> _P = 22.21%, <i>R</i> _{WP} = 20.55%, <i>R</i> _E = 19.04%							
(b)							
	Si/Al	192 i	−0.054 38(2)	0.03587(2)	0.124 64(2)	0.935(7)	192
	O(1)	96 h	0	−0.10610(4)	0.106 10(4)	1.61(4)	96
	O(2)	96 g	−0.002 20(5)	−0.00220(5)	0.141 72(7)	2.06(4)	96
	O(3)	96 g	0.176 30(5)	0.17630(5)	−0.033 72(7)	2.34(4)	96
	O(4)	96 g	0.178 19(5)	0.17819(5)	0.317 73(7)	2.04(4)	96
	Na(1)	32 e	0.234 13(4)	0.23413(4)	0.234 13(4)	2.56(7)	31.5(3)
	Na(2)	32 e	0.054 15(9)	0.05415(9)	0.054 15(9)	3.1(2)	15.8(3)
	Na(3)	16 c	0	0	0	5.3(4)	7.2(3)
<i>a</i> = 24.8096(0) Å, <i>R</i> _I = 4.68%, <i>R</i> _P = 9.08%, <i>R</i> _{WP} = 10.23%, <i>R</i> _E = 6.24%							

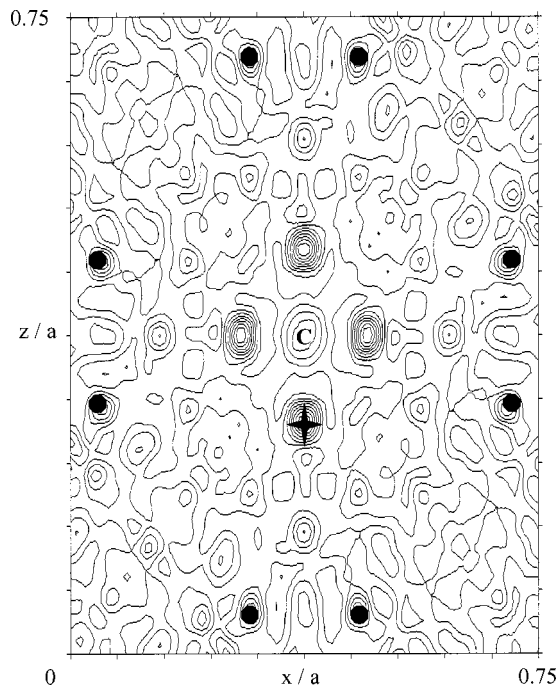


FIG. 3. Fourier difference map on the plane perpendicular to the $[0,1,0]$ axis about the center of the supercage located at $(3/8, 3/8, 3/8)$ for the observed intensities of the peaks for the diffraction pattern on zeolite loaded with ferrocene and those calculated for bare zeolite by Rietveld refinement, showing four iron atoms. The small dots represent the framework silicon/aluminum atoms, which lie in this plane (also indicated in Fig. 1), the C gives the center of the supercage. The cross on one of the iron atoms is also indicated in Fig. 1, and corresponds to the iron atom in the ferrocene molecule in Fig. 8.

Also, it has been shown before by means of Mössbauer experiments⁴ that at elevated temperatures a small fraction of the encaged ferrocene molecules diffuses out of the zeolite cages and forms a nonhomogeneous phase on the surface of the zeolite crystals. This could well have happened to our sample during storage. Therefore, it is likely that the observed diffuse scattering originates from ferrocene molecules on the outer surface of the zeolite crystals.

IV. DISCUSSION

There is a clear difference between the patterns for the bare NaY zeolite and the zeolite loaded with one or with two ferrocene molecules per zeolite supercage. Due to the higher scattering cross section for the ferrocene molecule as a whole this difference is more pronounced for the neutron diffraction patterns than for the x-ray patterns (the scattering of one ferrocene molecule per supercage amounts to 32% of the total scattering in case of neutron diffraction, and 11% in case of x-ray diffraction). In Fig. 6 we show part of the neutron diffraction pattern including the final fit on pure zeolite (top), the corresponding part of the neutron pattern with final fit on one ferrocene molecule per supercage (middle) and the corresponding part of the x-ray pattern with final fit on one ferrocene molecule per supercage (bottom). We have indicated some reflections to illustrate some differences between the three patterns. First there are differences in the relative intensities of the peaks between the neutron diffraction patterns on bare zeolite and on ferrocene in zeolite. One

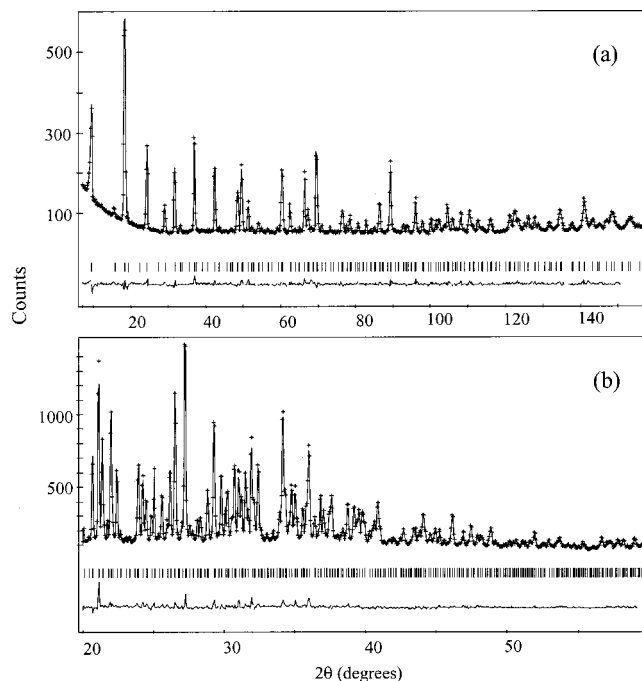


FIG. 4. Observed, calculated, and difference profiles for neutron powder diffraction (a) and x-ray powder diffraction (b) on NaY zeolite loaded with one ferrocene molecule per supercage.

can see, for example, that the intensity of the $(10, 8, 2)$ reflection is higher than the intensity of the $(9, 9, 3)$ reflection in case of the bare zeolite but lower in case of the loaded zeolite. The differences between the neutron and the x-ray diffraction patterns on ferrocene in zeolite are more pronounced. For example, the $(8, 8, 4)$ reflection is of low intensity in case of the neutron pattern, but is much more pronounced in the x-ray pattern. The same goes for the $(13, 5, 1)$, $(10, 10, 0)$, and $(10, 8, 2)$ reflections. Note that the distances between the various reflections shift a bit between the neutron and x-ray patterns because they are plotted as a function of 2θ instead of d spacing.

The adsorption of ferrocene molecules in NaY zeolite has only a small effect on the framework structure. One notable effect is a change in the lattice parameter (see also Table IV). Figure 7 compares part of the x-ray patterns on pure NaY zeolite and NaY zeolite loaded with one or two ferrocene molecules per supercage. One clearly sees a shift in the position of the peaks, corresponding to a change in the lattice parameter. We find for the bare zeolite a lattice parameter $a = 24.870$ Å determined from x-ray diffraction and $a = 24.815$ Å determined from neutron diffraction, which is within the range 24.60–25.12 Å which is typically found in the literature.⁷ After insertion of one ferrocene molecule per supercage the cell parameter decreases to $a = 24.767$ Å and 24.770 Å determined from x-ray and neutron diffraction, respectively. Upon insertion of two ferrocene molecules per supercage the cell parameter further decreases to $a = 24.706$ Å and $a = 24.713$ Å as found from x-ray and neutron diffraction. These slight decreases suggest an interaction between the adsorbed ferrocene molecules and the zeolite host. This effect has also been found for benzene in NaY zeolite⁷ and pi-complexes in Y-type zeolites.¹⁰ They suggest that this

TABLE II. Final parameters and R factors obtained from a Rietveld refinement on neutron (a) and x-ray (b) powder diffraction on NaY zeolite loaded with one ferrocene molecule per supercage.

	Atom	Position	x/a	y/a	z/a	B (\AA^2)	N
(a)							
	Si/Al	192 i	-0.0548(2)	0.0359(2)	0.1254(2)	0.40(7)	192
	O(1)	96 h	0	-0.1062(2)	0.1062(2)	1.1(1)	96
	O(2)	96 g	-0.0025(2)	-0.0025(2)	0.1439(2)	1.8(2)	96
	O(3)	96 g	0.1782(2)	0.1782(2)	-0.0332(3)	2.9(2)	96
	O(4)	96 g	0.1760(2)	0.1760(2)	0.3192(3)	2.4(2)	96
	Na(1)	32 e	0.2355(4)	0.2355(4)	0.2355(4)	1.7(5)	30(1)
	Na(2)	32 e	0.0591(7)	0.0591(7)	0.0591(7)	2(1)	13(1)
	Na(3)	16 c	0	0	0	1(1)	6.4(6)
	Fe	48 f	0.375	0.375	0.2705(3)	1.0(6)	7.54(4)
	C(1)	96 g	0.3276	0.3276	0.3201(3)	3.3(3)	15.08(8)
	C(2)	192 i	0.2943	0.3609	0.2858(3)	3.3(3)	30.2(2)
	C(3)	192 i	0.3070	0.3482	0.2305(3)	3.3(3)	30.2(2)
	D(1)	96 g	0.3276	0.3276	0.3648(3)	6.4(3)	15.08(9)
	D(2)	192 i	0.2642	0.3910	0.2997(3)	6.4(3)	30.2(2)
	D(3)	192 i	0.2884	0.3668	0.1942(3)	6.4(3)	30.2(2)
$a = 24.7697(2)$ \AA , $R_I = 6.70\%$, $R_P = 16.81\%$, $R_{WP} = 14.93\%$, $R_E = 10.47\%$							
(b)							
	Si/Al	192 i	-0.053 97(2)	0.035 87(2)	0.124 30(2)	0.662(4)	192
	O(1)	96 h	0	-0.106 16(5)	0.106 16(5)	1.34(5)	96
	O(2)	96 g	-0.002 39(6)	-0.002 39(6)	0.143 71(7)	1.54(4)	96
	O(3)	96 g	0.177 57(6)	0.177 57(6)	-0.03270(8)	1.93(4)	96
	O(4)	96 g	0.176 74(6)	0.176 74(6)	0.318 59(9)	1.31(4)	96
	Na(1)	32 e	0.236 54(4)	0.236 54(4)	0.236 54(4)	2.65(7)	33.2(3)
	Na(2)	32 e	0.0560(1)	0.0560(1)	0.0560(1)	2.1(2)	14.8(3)
	Na(3)	16 c	0	0	0	1.6(2)	7.7(2)
	Fe	48 f	0.375	0.375	0.2718(1)	2.6(2)	7.6(1)
	C(1)	96 g	0.3276	0.3276	0.3214(1)	5.6(3)	15.2(2)
	C(2)	192 i	0.2943	0.3609	0.2871(1)	5.6(3)	30.4(4)
	C(3)	192 i	0.3070	0.3482	0.2318(1)	5.6(3)	30.4(4)
$a = 24.7669(0)$ \AA , $R_I = 3.69\%$, $R_P = 8.25\%$, $R_{WP} = 9.69\%$, $R_E = 6.70\%$							

TABLE III. Final parameters and R factors obtained from a Rietveld refinement on neutron (a) and x-ray (b) powder diffraction on NaY zeolite loaded with two ferrocene molecules per supercage.

	Atom	Position	x/a	y/a	z/a	B (\AA^2)	N
(a)							
	Si/Al	192 i	-0.0541(2)	0.0360(2)	0.1249(2)	0.55(9)	192
	O(1)	96 h	0	-0.1052(2)	0.1052(2)	2.2(2)	96
	O(2)	96 g	-0.0034(2)	-0.0034(2)	0.1450(2)	1.9(2)	96
	O(3)	96 g	0.1785(2)	0.1785(2)	-0.0330(3)	3.4(2)	96
	O(4)	96 g	0.1756(2)	0.1756(2)	0.3186(3)	3.0(2)	96
	Na(1)	32 e	0.2397(4)	0.2397(4)	0.2397(4)	4.9(5)	34(1)
	Na(2)	32 e	0.060(1)	0.060(1)	0.060(1)	4.9(5)	15(1)
	Na(3)	16 c	0	0	0	4.9(5)	10.2(7)
	Fe	48 f	0.375	0.375	0.2707(2)	1.3(4)	12.2(2)
	C(1)	96 g	0.3276	0.3276	0.3203(2)	2.2(2)	24.4(3)
	C(2)	192 i	0.2943	0.3609	0.2860(2)	2.2(2)	48.8(7)
	C(3)	192 i	0.3070	0.3482	0.2307(2)	2.2(2)	48.8(7)
	D(1)	96 g	0.3276	0.3276	0.3650(2)	4.7(2)	24.4(3)
	D(2)	192 i	0.2642	0.3910	0.2998(2)	4.7(2)	48.8(7)
	D(3)	192 i	0.2884	0.3668	0.1944(2)	4.7(2)	48.8(7)
$a = 24.7129(2)$ \AA , $R_I = 7.51\%$, $R_P = 17.64\%$, $R_{WP} = 16.42\%$, $R_E = 11.58\%$							
(b)							
	Si/Al	192 i	-0.053 78(3)	0.035 90(3)	0.124 14(4)	0.71(1)	192
	O(1)	96 h	0	-0.106 28(8)	0.106 28(8)	1.66(7)	96
	O(2)	96 g	-0.002 71(9)	-0.002 71(9)	0.1445(1)	1.37(7)	96
	O(3)	96 g	0.1781(1)	0.1781(1)	-0.0323(1)	2.02(7)	96
	O(4)	96 g	0.175 94(9)	0.175 94(9)	0.3196(1)	1.38(7)	96
	Na(1)	32 e	0.240 03(7)	0.240 03(7)	0.240 03(7)	2.7(1)	35.1(4)
	Na(2)	32 e	0.0584(2)	0.0584(2)	0.0584(2)	2.0(3)	12.4(4)
	Na(3)	16 c	0	0	0	0.4(3)	7.1(3)
	Fe	48 f	0.375	0.375	0.2715(1)	2.2(1)	14.6(2)
	C(1)	96 g	0.3276	0.3276	0.3210(1)	3.9(2)	29.2(4)
	C(2)	192 i	0.2943	0.3609	0.2868(1)	3.9(2)	58.4(8)
	C(3)	192 i	0.3070	0.3482	0.2315(1)	3.9(2)	58.4(8)
$a = 24.7064(1)$ \AA , $R_I = 4.18\%$, $R_P = 13.29\%$, $R_{WP} = 15.16\%$, $R_E = 9.38\%$							

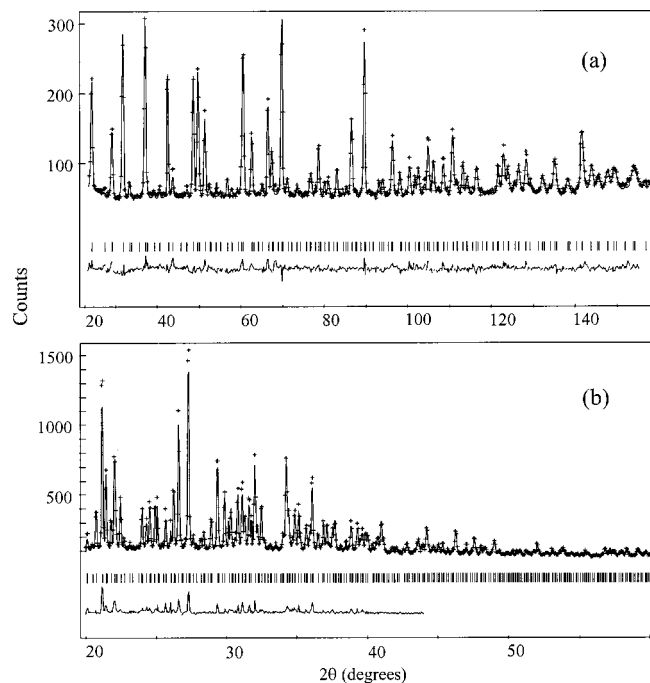


FIG. 5. Observed, calculated, and difference profiles for neutron powder diffraction (a) and x-ray powder diffraction (b) on NaY zeolite loaded with two ferrocene molecules per supercage.

stems from an interaction between the ions in the zeolite and the pi-electrons of the adsorbed molecules. Indeed we find that for a loading of one ferrocene molecule per supercage the sodium ions at the SII sites shift with 0.083 Å and 0.11 Å for x-ray and neutrons, respectively, towards the center of the supercage, suggesting an interaction between these ions and the cyclopentadienyl rings of the ferrocene molecule. The positions of the sodium ions at the SII sites for loadings of two ferrocene molecules per supercage show an increased shift towards the center of the zeolite supercage, with 0.21 and 0.27 Å compared with the bare zeolite for x-ray and neutrons, respectively. Note that now all sodium ions at the SII sites interact with a ferrocene molecule, whereas in the case of one ferrocene molecule this is on average only half of the sodium ions at these sites. This migration of the sodium cations at the SII sites has also been found for benzene in NaY zeolite, where it was by 0.09 Å for loadings of 2.6 benzene molecules per supercage.⁷

Figure 8 depicts the final result for the position and orientation of the ferrocene molecules in the zeolite supercage. Note that the position of the iron atom of the ferrocene molecule corresponds to the cross in Figs. 1 and 3. The iron atom is on a 48f site, which is on the crossing of two symmetry planes, one parallel to the ferrocene rings through the iron atom, the other perpendicular to the first one, right through the rings. The top carbon and hydrogen (or deuterium) atoms are on a 96g site, the other ones on a general 192i site. With this symmetry only three carbon and three hydrogen or deuterium atoms are needed to fully describe both cyclopentadienyl rings of the ferrocene molecule in the zeolite supercage. The distance between the center of the ring and the sodium ion is approximately 3.18 Å for a ferrocene molecule, whereas it is 2.7 Å for a benzene molecule. For the case of

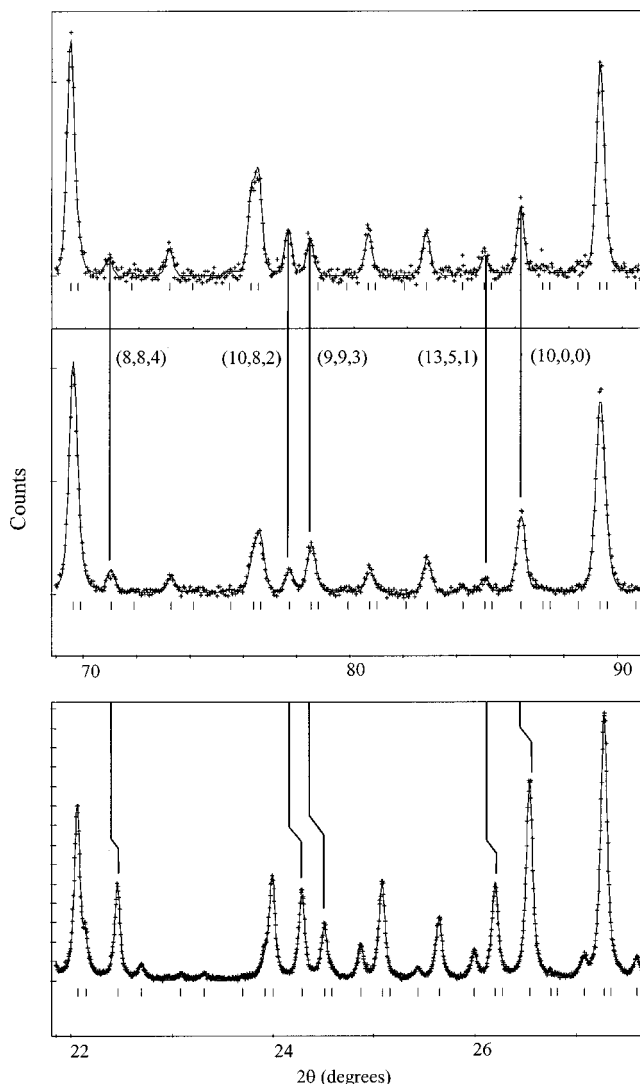


FIG. 6. Part of the neutron diffraction pattern including the final fit on pure zeolite (top), the corresponding part of the neutron pattern with final fit on one ferrocene molecule per supercage (middle), and the corresponding part of the x-ray pattern with final fit on one ferrocene molecule per supercage (bottom) showing the differences in relative intensity of the reflections.

two ferrocene molecules per zeolite supercage the second molecule is situated in the same way as the first one, between the two other sodium ions at the SII positions on the surface of the supercage. Note that the z -axis in the figure corresponds to the z -axis used in the refinement.

There is no indication that the rings take another orientation than we found, or that they are disordered with respect

TABLE IV. Lattice parameter, a , as found from Rietveld refinements on x-ray and neutron diffraction patterns for bare NaY zeolite and NaY zeolite loaded with one or two ferrocene molecules per supercage. The estimated standard deviations incorporate the error in incident wavelengths.

	a (nm) x-ray	a (nm) neutron
Bare NaY	24.810(1)	24.815(10)
+1 ferrocene	24.767(1)	24.770(10)
+2 ferrocene	24.706(1)	24.713(10)

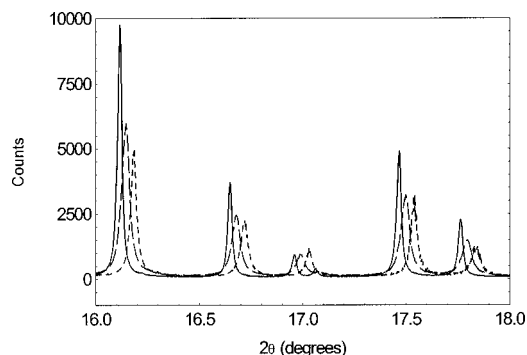


FIG. 7. Part of the x-ray patterns on pure NaY zeolite (solid line), and NaY zeolite loaded with one (dashed line) or two (dotted line) ferrocene molecules per supercage showing the decrease in lattice parameter upon adsorption of ferrocene molecules in NaY zeolite.

to each other. Refining the diffraction patterns of ferrocene in zeolite with the rings “upside down” gave notably worse results.

We have also refined the neutron diffraction patterns with the positions of all carbon atoms and deuterium atoms as free parameters. This improves the agreement between the observed and calculated patterns by about 5%. However, the shape of the ferrocene molecule is actually indistinguishable from the starting shape as above because this falls well within the error bars of the positions of the atoms in the ferrocene molecule.

To show that the ferrocene molecule is indeed in an energy minimum on the position in the zeolite supercage as found above we perform *ab initio* calculations using density functional theory using the module Dmol³ of the program CERIUS².¹¹ For this we optimize the geometry and position of a ferrocene molecule surrounded by a zeolite supercage fragment. The model we use consists of one ferrocene molecule, two sodium cations and part of the zeolite supercage framework as shown in Fig. 9. The positions of the atoms are taken from the Rietveld refinement on the neutron diffraction data on one ferrocene molecule per supercage. The oxygen atoms adjacent to the silicon/aluminum atoms are replaced by hydrogen atoms to preserve the electroneutrality of the model. The positions of these terminal hydrogens are fixed during

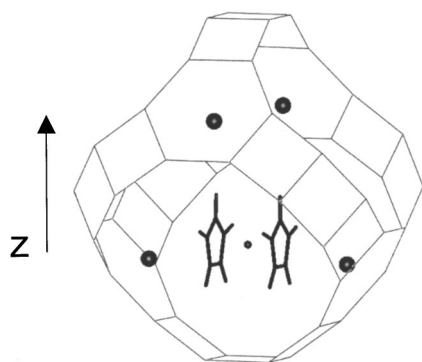


FIG. 8. Location of a ferrocene molecule in the supercage of NaY zeolite. The large dots show the four sodium ions in the supercage forming a tetrahedron, and are also shown in Fig. 1. The iron atom of the ferrocene molecule is indicated by a cross in Figs. 1 and 3. Note the large free volume in the supercage above the ferrocene molecule accessible to other molecules.

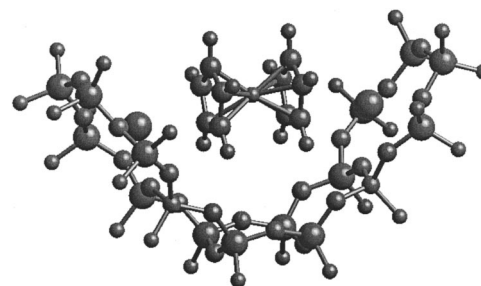


FIG. 9. Model of a ferrocene molecule inside a zeolite supercage used for DFT calculations.

the geometry optimization. The positions of all the other atoms are allowed to vary. We use the local density approximation, Perdew Wang functionals, the DND basis set,¹¹ and an atomic cutoff radius of 5.5 Å.

After optimization of the geometry we find that the hydrogen atoms of the ferrocene molecule are tilted with about 1.3° from the C₅ rings towards the Fe atom, a trend which is also found with measurements on pure ferrocene¹² or with DFT calculations on a single ferrocene molecule.^{9,13} The ferrocene molecule as a whole virtually stays at the same position, and there are no significant changes in the zeolite fragment. The structure found from the refinements indeed corresponds to an energy minimum.

The difference in total energy between the bare fragment added with the total energy of a single ferrocene molecule as calculated before⁹ and the fragment with a ferrocene molecule amounts to -130 kJ mol^{-1} . This compares well with the measured sorption energy of benzene molecules in NaY zeolite, which is around -77 kJ mol^{-1} .¹⁴

The question arises as to what interactions are responsible for the found position of the ferrocene molecule. The cyclopentadienyl rings of the ferrocene molecule are slightly negatively charged. Since the sodium ions are positively charged it seems natural that the rings orient towards them by electrostatic interactions between the π -systems of the aromatic rings and the ions, as with benzene.⁷ In solid ferrocene the rings are rotated by 9° from the eclipsed orientation, where the rings are just on top of each other.¹² When adsorbed in a zeolite, the ferrocene rings take the eclipsed orientation. The C–O distance via the hydrogen atom in the ferrocene ring amounts to 5.58 Å, while the angle is 144.8° (see also Table V). These values are typical for CH–O interactions.¹⁵ Former DFT calculations on a single ferrocene molecule show that the energy difference for rotation of the rings from 9° to 0° is almost zero,⁹ and rather weak hydrogen bonds could well explain the eclipsed ring orientation of ferrocene in zeolite Y. The Coulombic interaction between the

TABLE V. Closest contacts between C and H atoms of the ferrocene molecule and O and Na atoms of the zeolite framework.

	Distance (Å)
H–O	2.63(1)
C–Na	3.23(1)
C–O	3.56(1)

π -systems of the aromatic rings and the sodium ions would be optimized if the ferrocene molecule would lie on the line connecting the two sodium ions on the supercage wall. Moreover, this would also lead to considerably shorter hydrogen bonds. Currently we are investigating the question why the ferrocene molecule lies almost 1 Å above the line connecting the sodium ions.

Apart from the slight reorientation of the rings, the geometry of the ferrocene molecule barely changes. However, the reactivity is dramatically increased. In general, the reactivity of molecules in zeolites can be increased by the weakening bonds by host/guest interactions, or by holding reactants in close proximity with each other. The barely changed ferrocene geometry suggests that the latter is the case. Inspection of Figs. 8 and 9 reveals a large “free volume” on the expected side of the ferrocene molecule, which is an attractive site for any potential reactants.

V. CONCLUSIONS

We have shown that ferrocene molecules adsorbed in the supercages of NaY zeolite are located just above a line joining two neighboring sodium ions at the SII positions in the zeolite supercage for loadings of one or two ferrocene molecules per supercage. The cyclopentadienyl C_5H_5 rings are oriented towards the sodium ions in an ordered manner. The inclusion of ferrocene in a Y-type zeolite thus provides a homogeneous distribution of iron throughout the zeolite at well-defined locations. We have shown this position to be an energy minimum using density functional theory. Also, the unit cell of the zeolite contracts upon adsorption of ferrocene.

The main interactions between a ferrocene molecule and the zeolite framework are Coulombic interactions that pull the ferrocene molecule between two sodium ions. Furthermore, H-bonds are responsible for the ordered ring orienta-

tion. Besides the ring reorientation, the geometry of ferrocene in NaY zeolite is barely different from the solid state. The increased reactivity must thus be an effect of the position of ferrocene, which renders it vulnerable to attack.

With x-ray scattering heavy atoms such as the iron atom in ferrocene are easy to locate due to their high scattering. Lighter atoms, such as for example carbon and hydrogen in the cyclopentadienyl rings of ferrocene, are much harder to locate. Carbon and deuterium atoms are clearly visible in the neutron diffraction patterns, making an accurate determination of the orientation of the cyclopentadienyl rings possible. The combination of both x-ray and neutron powder diffraction could also prove very useful for localizing other transition metal complexes in zeolites with potential applications in, e.g., catalysis.

¹G. A. Ozin and C. Gil, *Chem. Rev.* **89**, 1749 (1989).

²W. M. H. Sachtler and Z. Zhang, *Adv. Catal.* **39**, 129 (1993).

³T. Bein, *Comprehensive Supramolecular Chemistry*, 1st ed., edited by J. L. Atwood, J. E. D. Davies, D. D. MacNicol, and F. Vögtle (Elsevier Science, New York, 1996), Vol. 7, Chap. 20.

⁴A. R. Overweg, H. Koller, J. W. de Haan, L. J. M. van de Ven, A. M. van der Kraan, and R. A. van Santen, *J. Phys. Chem. B* **103**, 4298 (1999).

⁵E. Kemner, I. M. de Schepper, A. J. M. Schmets, H. Grimm, A. R. Overweg, and R. A. van Santen, *J. Phys. Chem. B* **104**, 1560 (2000).

⁶A. Jouanneaux, WinMProf: a visual Rietveld Software, ICP Newsletter, “Commission on Powder Diffraction” **21**, 13 (1999).

⁷A. N. Fitch, H. Jovic, and A. Renouprez, *J. Phys. Chem.* **90**, 1311 (1986).
⁸[ftp://charybde.saclay.cea.fr/pub/divers/progs_pc/fourier/](http://charybde.saclay.cea.fr/pub/divers/progs_pc/fourier/)

⁹E. Kemner, I. M. de Schepper, G. J. Kearley, and U. A. Jayasooriya, *J. Chem. Phys.* **112**, 10926 (2000).

¹⁰M. Czjzek, H. Fuess, and T. Vogt, *J. Phys. Chem.* **95**, 5255 (1991).

¹¹B. Delley, *J. Chem. Phys.* **508**, 92 (1990).

¹²P. Seiler and J. D. Dunitz, *Acta Crystallogr., Sect. B: Struct. Sci.* **35**, 2020 (1994).

¹³A. Bérces, T. Ziegler, and L. Fan, *J. Phys. Chem.* **98**, 1584 (1994).

¹⁴S. M. Auerbach, L. M. Bull, N. J. Henson, H. I. Metiu, and A. K. Cheetham, *J. Phys. Chem.* **100**, 5923 (1996).

¹⁵U. Koch and P. L. A. Popelier, *J. Phys. Chem.* **99**, 9747 (1995).